

MIT Open Access Articles

A new twist on glass: A brittle material enabling flexible integrated photonics

The MIT Faculty has made this article openly available. **Please share** how this access benefits you. Your story matters.

Citation: Li, Lan et al. "A New Twist on Glass: A Brittle Material Enabling Flexible Integrated Photonics." *International Journal of Applied Glass Science* 8, 1 (December 2016): 61–68 © 2016 The American Ceramic Society and Wiley Periodicals, Inc

As Published: <http://dx.doi.org/10.1111/ijag.12256>

Publisher: Wiley Blackwell

Persistent URL: <http://hdl.handle.net/1721.1/112637>

Version: Author's final manuscript: final author's manuscript post peer review, without publisher's formatting or copy editing

Terms of use: Creative Commons Attribution-Noncommercial-Share Alike



A new twist on glass: a brittle material enabling flexible integrated photonics

Lan Li¹, Hongtao Lin¹, Jerome Michon¹, Yizhong Huang¹, Junying Li¹, Qingyang Du¹, Anupama Yadav², Kathleen Richardson², Tian Gu¹, and Juejun Hu^{1*}

¹Department of Materials Science & Engineering, Massachusetts Institute of Technology,
Cambridge, Massachusetts 02139, USA

²College of Optics and Photonics, CREOL, Department of Materials Science and Engineering,
University of Central Florida, Orlando, Florida 32816, USA

*hujuejun@mit.edu

Abstract

Glass is in general brittle and therefore usually cannot sustain large deformation. Recent advances in glass material development as well as micro-mechanical designs, however, are set to defy the conventional wisdom through the demonstration of flexible integrated photonics that can be bent, twisted, and even stretched without compromising its structural integrity and optical performance. In this paper, we review the latest progress in this emerging field, and discuss the rational material and mechanical engineering principles underlying the extraordinary flexibility of these photonic structures. Leveraging these design strategies, we demonstrated bendable chalcogenide glass waveguide circuits, flexible glass waveguide-integrated nanomembrane photodetectors, and stretchable glass photonics.

Introduction

Since the first proposal of integrated photonic circuits by S. Miller in 1969 [1], integrated photonics, which involves a multitude of miniaturized optical components connected by an optical waveguide network on one single substrate, has thrived over the past decades and is now widely regarded as a transformative paradigm shift in optics and photonics analogous to integrated circuits revolutionizing the electronic industry. Whether it is the archetypal “laser beam circuitry” on a glass plate envisaged by S. Miller or state-of-the-art photonic chips diced from a silicon or InP wafer, integrated photonics platforms demonstrated thus far are pre-dominantly fabricated on rigid substrates. What if we can make flexible integrated photonic devices that can be bent, twisted, and stretched?

The success paradigm of flexible electronics, a close analogy of flexible photonics, provides a convincing answer. Flexible electronics, which dates back to the 1960s [2], is now a booming 5.13 billion US dollar market with a projected compound annual growth rate (CAGR) of 21% [3]. Compared to traditional electronic components integrated on rigid substrates, their flexible counterparts are often lighter, more compact and more durable (with improved impact resistance), and are therefore witnessing rapidly increasing adoption in consumer electronic products. The mechanical compliance of flexible electronics enables conformal integration on biological tissues such as human skin for continuous health monitoring [4], as well as minimally invasive implantable medical devices with significantly reduced risk of tissue damage [5]. Flexible devices are also compatible with roll-to-roll (R2R) manufacturing, an extremely high-throughput, cost-effective solution to large-area applications such as photovoltaics and display. In the same vein, flexible photonics is starting to reap these benefits: for instance, R2R printed flexible optical waveguide sensors now claim drastically reduced cost ideal for single-use/disposable applications with production length up to hundreds of meters [6, 7].

In addition to the processing and deployment advantages already well-recognized in the flexible electronics community, adding photonics into the picture further furnishes numerous intriguing opportunities beyond the current capabilities of flexible electronics. Light is the preferred carrier for ultra-high bandwidth data communications and is inherently immune to electromagnetic interference (EMI); spectroscopic signatures extracted from optical measurements provide unambiguous information about chemical species; and there are also many applications which rely on light-matter interactions and inevitably involves photonics technologies, such as lighting, imaging, and display. As one specific application example leveraging the unique benefits of photons, flexible optical waveguides are currently being pursued for board-level data communications to replace conventional electrical interconnects in order to improve datacenter energy efficiency and bandwidth density, where their mechanical flexibility facilitates high-density, low-cost packaging and assembly [8-12]. Flexible and stretchable photonic structures can also be conformally integrated on arbitrary curvilinear optical surfaces to impart unconventional functions (e.g., aberration compensation) to the optical element underneath [13, 14]. Last but not least, mechanical deformation presents a simple and elegant approach for broadband photonic device tuning and reconfiguration [15-18].

First flexible photonic devices were fabricated using polymers exploiting the inherent mechanical flexibility of organic polymer materials [19-22]. These all-polymer devices, however, suffer from several drawbacks. In terms of optical properties, the accessible range of refractive indices in common optical polymers is limited to 1.45-1.7 [23], posing a severe constraint on photonic designs. The presence of C-H bonds in many polymers causes parasitic optical absorption in the near-infrared due to the chemical bond's 2nd and 3rd order vibrational overtones [23]. From

a device processing perspective, few polymers can withstand high processing temperatures ($> 400\text{ }^{\circ}\text{C}$), which limits their integration capacity with other material systems. Furthermore, the inferior optoelectronic properties of polymers largely prohibit their applications in active components. Therefore, unleashing the full potential of flexible photonics mandates further expansion of its material repertoire beyond organic polymers. Crystalline semiconductors such as Si overcome these disadvantages of polymers. By thinning semiconductor wafers to sub-micron thickness and transferring the resulting semiconductor nanomembranes (NMs) onto supporting polymer substrates, the NM structures can be made flexible [24-28]. The hybrid NM transfer process, however, limits the yield and throughput of the approach. In addition, NM photonic devices exhibit only moderate flexibility with a bending radius typically no less than 5 mm and cannot handle stretching deformation.

Glass, traditionally regarded as a fragile substance, is a somewhat surprising candidate in the search for next-generation materials for flexible integrated photonics. In the past few years, major advances in glass material development as well as micro-mechanical designs have given birth to a suite of glass-based flexible photonic devices which harness the useful properties of glass while circumventing its brittleness. Two types of glass-based flexible photonic systems have been developed. The first class of devices are fabricated on ultra-thin ($100\text{ }\mu\text{m}$ or less in thickness) flexible glass substrates now commercially available through several vendors (e.g., Willow[®] Glass from Corning, AF 32[®] eco Glass from Schott, SPOOL[®] Glass from Asahi, and G-Leaf[®] Glass from NEG). These glass products, most often made of alkali-free borosilicates, derive their mechanical flexibility from both reduced glass thickness and enhanced material strength. When bent to a given radius, the surface stress scales inversely with the glass sheet thickness: with a minimum thickness of $25\text{ }\mu\text{m}$, state-of-the-art ultra-thin glass sheets can be bent to a radius of 1 cm or even less. The traditional float glass technology is no longer capable of producing glass sheets with such a small thickness, and therefore manufacturers turned to down draw techniques for the ultra-thin glass production [29]. Another critical benefit of the down draw methods is the superior product surface quality: since the glass sheets are not in contact with molten metal bath during forming, the down draw processes render the products with a pristine surface finish. To further suppress surface defect generation that compromises mechanical strength, a set of special handling protocols are implemented to glass cleaning, cutting, and lamination, and the end product surfaces and edges can be protected with polymer coatings or chemically strengthened via ion exchange [30]. Compared to polymers, ultra-thin glass features several advantages as a substrate material for flexible electronics and photonics, including their exceptional thermal and chemical stability as well as low permeation rates for ambient gases and water. As an example of this type of glass flexible photonic devices, Fig. 1a shows an optical waveguide inscribed in a Willow[®] Glass substrate using ultrafast laser direct writing (LDW) [31]. The authors demonstrated waveguide writing in glass substrates with thicknesses ranging from $100\text{ }\mu\text{m}$ down to $25\text{ }\mu\text{m}$, and the fabricated waveguides exhibit low propagation loss in the range of 0.1 to 0.25 dB/cm at 1550 nm wavelength. Bending radius of the flexible waveguides is limited to $\sim 1.5\text{ cm}$ by radiative loss due to the small index contrast induced by laser modification ($\Delta n \sim 5 \times 10^{-3}$). Higher index contrast is attainable with LDW, although the authors suggest that an optical loss penalty results from the ensuing significant structural damage in glass induced by laser writing. Lastly, while silicate glass is the mainstream material for ultra-thin flexible glass substrates, the recent demonstration of low-loss ($< 0.15\text{ dB/cm}$ at 1550 nm) laser-written waveguides in flexible As_2S_3 glass tapes (Fig. 1b) indicates that soft glasses, usually thought of having inferior mechanical properties compared to silicates, can also be processed in a highly flexible and rugged form [32].

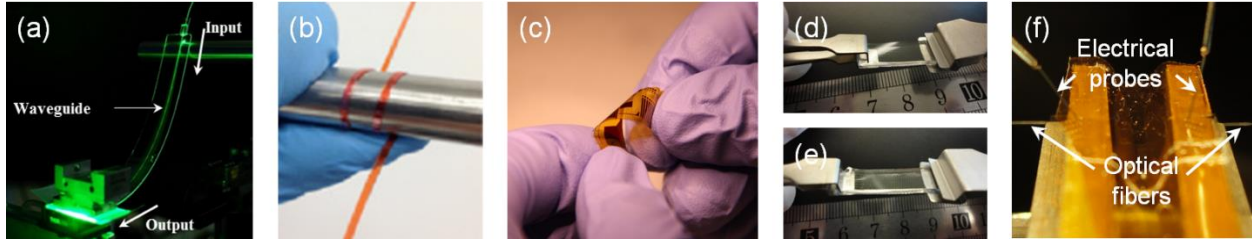


Fig. 1. Examples of glass-based planar flexible photonic devices: (a) a laser-inscribed waveguide in Willow[®] Glass [31]; (b) a 250 μm thick As_2S_3 tape wrapped around a rod of 6.35 mm radius [32]; (c) a bendable ChG waveguide-resonator chip [33]; (d) & (e) stretchable ChG photonics [34]; (f) flexible ChG waveguide-integrated nanomembrane photodetectors under bending test [35].

Further improved mechanical robustness and optical confinement have been achieved following the second approach, where photonic devices are fabricated in glass thin films deposited on flexible polymer substrates. In this case, mechanical flexibility of the glass-polymer hybrid structures primarily benefits from shrewd configurational designs which minimize strains exerted on glass devices during deformation [28, 36]. Chalcogenide glasses (ChGs), the amorphous compounds of S, Se, and/or Te, are particularly attractive for this application, since they can be monolithically deposited and processed at low temperatures ($< 200\text{ }^\circ\text{C}$) on organic polymer substrates, and their high refractive indices ($n > 2$) provide strong optical confinement, allowing tight bends with minimal radiative loss. Besides ChGs, several amorphous thin film materials (which are not classical glasses) such as TiO_2 and a-Si also claim some of the aforementioned advantages of ChGs and have been used in flexible photonics fabrication [37, 38]. Following the approach, we have demonstrated a series of flexible photonic devices shown in Fig. 1c-f which we review in the following sections [18, 33-35, 39, 40].

Bend, but don't break: multi-neutral-axis design enabled foldable ChG photonics

Fig. 2a illustrates the generic fabrication process of passive ChG flexible photonic devices. The process starts with coating an epoxy polymer (SU8 negative resist, MicroChem Corp.) layer on a rigid handler substrate (oxide coated Si wafer), followed by evaporation deposition and lithographic patterning of ChG thin films to define the photonic devices. Substrate heating measured during ChG film deposition is negligible ($< 5\text{ }^\circ\text{C}$ for $\text{Ge}_{23}\text{Sb}_7\text{S}_{70}$ glass) and thus the substrate is maintained at near room temperature throughout the process. 2.5-D multi-layer structures can also be fabricated simply by repeating the epoxy-coating/deposition/patterning steps: the excellent planarization capability of SU-8 epoxy ensures high pattern fidelity during subsequent lithographic steps not affected by underlying topology from device layers underneath. The monolithic process circumvents the need to transfer devices between different substrates to significantly improve the fabrication yield and throughput and is compatible with standard semiconductor microfabrication technologies. In the last step, the photonic devices are delaminated from the handler substrate using a Kapton tape to form free-standing flexible structures.

Fig. 2c illustrates the layer structure of the resulting flexible chip. Since the bi-layer Kapton tape consists of a silicone rubber adhesive film and a polyimide substrate, the delaminated flexible chip assumes an “Oreo” geometry with the soft silicone layer (Young's modulus $\sim 1\text{ MPa}$) sandwiched between two stiff layers (the Young's moduli of polyimide and SU-8 are both $\sim 2\text{ GPa}$). Interestingly, we have identified that the classical multilayer beam bending theory fails to

provide a correct strain distribution in the structure. This is because significant shear deformation is introduced in the soft silicone layer upon bending due to the large elastic modulus mismatch between the layers, which violates the assumption that cross-sectional planes remain planar after bending underlying the classical bending theory. We have therefore derived a new multi-neutral-axis (MNA) theory taking into account the effect and the analytical MNA framework has been validated through finite element simulations (Fig. 2b) as well as our strain-optical coupling measurements [39].

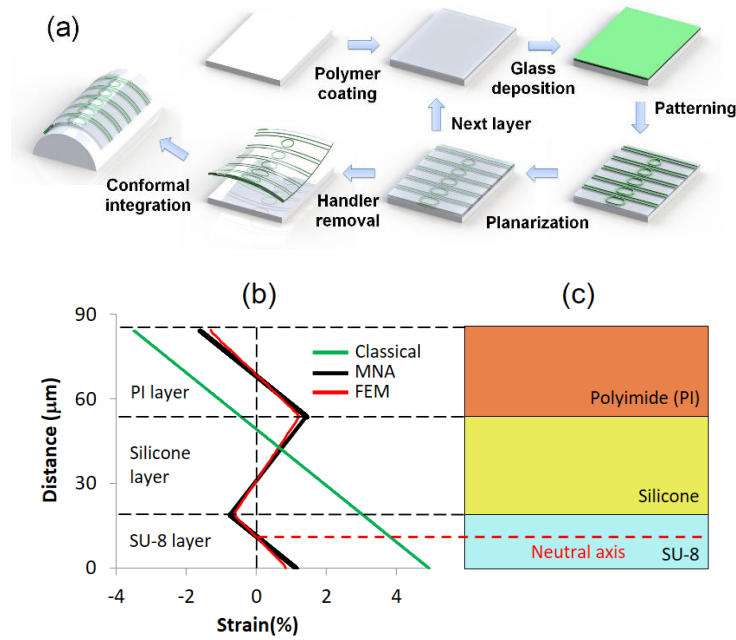


Fig. 2. (a) Fabrication process sequence of passive flexible photonic devices; (b) strain distribution in the flexible structure calculated using the classical multilayer bending theory, the multi-neutral-axis (MNA) theory and finite element method (FEM) simulations; (c) schematic cross-sectional structure of the flexible photonic structure after delamination: the red dotted line indicates the location of the neutral axis in the SU-8 layer [39].

The new MNA theory specifies that a neutral axis emerges in the SU-8 layer where the strains vanish. Consequently, the structure can readily accommodate large bending deformations without damaging the devices by placing the glass devices at the neutral axis. The configuration further allows significant degrees of freedom in device engineering. Unlike the classical bending theory which stipulates a single neutral axis near the center of the entire multilayer stack, the location of the neutral axis in SU-8 can be flexibly tuned by adjusting the layer thicknesses and moduli in the laminated structure such that the optical devices can be placed at difference locations to meet specific application needs.

Following the MNA design, we have demonstrated foldable $\text{Ge}_{23}\text{Sb}_7\text{S}_{70}$ ChG optical devices boasting both record optical performance and extraordinary mechanical flexibility. Fig. 3a is a histogram showing the distribution of intrinsic optical quality factors (Q-factors) in flexible $\text{Ge}_{23}\text{Sb}_7\text{S}_{70}$ micro-disk resonators measured near 1550 nm wavelength. Our best device exhibited a Q-factor of 4.6×10^5 , the highest value reported for photonic devices on plastic substrates. To test the mechanical reliability of the flexible devices, optical transmittance of the resonators was measured after repeated bending cycles with a bending radius of 0.5 mm. Fig. 3b shows that there

were minimal variations in Q-factor and extinction ratio after multiple bending cycles. The device therefore far outperforms traditional flexible photonic components based on semiconductor NMs or those integrated on ultra-thin glass substrates which can only sustain bending radius down to several millimeters.

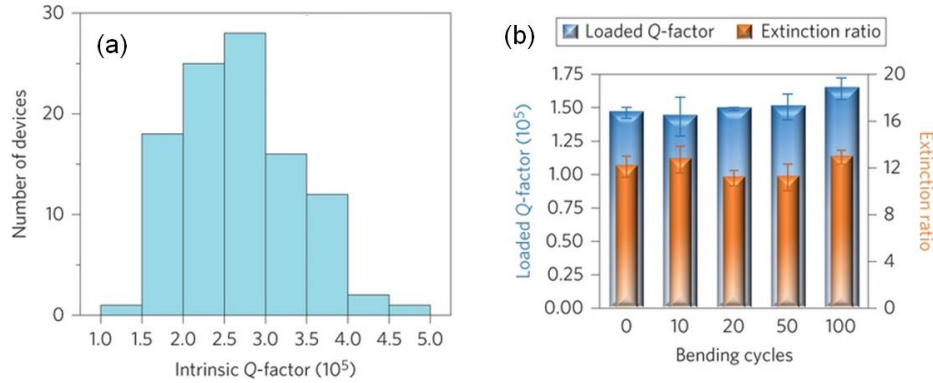


Fig. 3. (a) Q-factor distribution measured in flexible micro-disk resonators; (b) Q-factors and extinction ratios of the resonator after multiple bending cycles at a bending radius of 0.5 mm [39].

Stretchable integrated photonics

A truly flexible photonic module ought to be both bendable and stretchable. The ability of a functional substrate to tolerate stretching deformation is essential for wrinkle-free conformal integration on general curvilinear surfaces (e.g. spherical surfaces), which is also mandatory for epidermal sensors, as human skin exhibits stretchability up to 20%. Using epoxy polymers as the substrate supports bending to sub-millimeter radius as we discussed in the preceding section, however precludes stretching deformation. Instead, elastomers are the only practical substrate options for simultaneously bendable and stretchable photonics [41].

Photonic integration on elastomer substrates, however, presents a severe technical barrier. First of all, elastomers are known for their gigantic coefficient of thermal expansion (CTE). For example, polydimethylsiloxane (PDMS) has a CTE of 310 ppm, far greater than that of Si (2.6 ppm) or Ge₂₃Sb₇S₇₀ glass (20.8 ppm). High-quality optical thin film deposition directly on PDMS is therefore not possible due to the large CTE mismatch. The CTE mismatch also leads to resist film cracking and poor pattern fidelity. Secondly, while elastomers are highly stretchable, most optical materials cannot sustain tensile strain of more than a few percent. Last but not least, stretching results in geometric deformation of photonic components which inevitably modifies their optical responses. Such changes destabilize device operation, in particular for applications such as sensing where a stable baseline is of paramount importance.

To address these challenges, we have devised a strategy combining both material engineering and micro-mechanical design. We chose Ge₂₃Sb₇S₇₀ glass as our main optical material, given its good chemical and thermal stability (compared to the archetypal ChG compositions As₂S₃ and As₂Se₃ which are prone to surface oxidation [42]), low deposition temperature, as well as established low loss optical performance [43]. The device fabrication process follows that in Fig. 2a. During the polymer coating step, a PDMS film and an SU-8 layer are sequentially spin coated. The PDMS layer functions as the substrate, whereas SU-8, having an intermediate CTE of 52 ppm, is sandwiched between Ge₂₃Sb₇S₇₀ glass and PDMS to relieve thermal stress caused by the CTE mismatch between PDMS and glass.

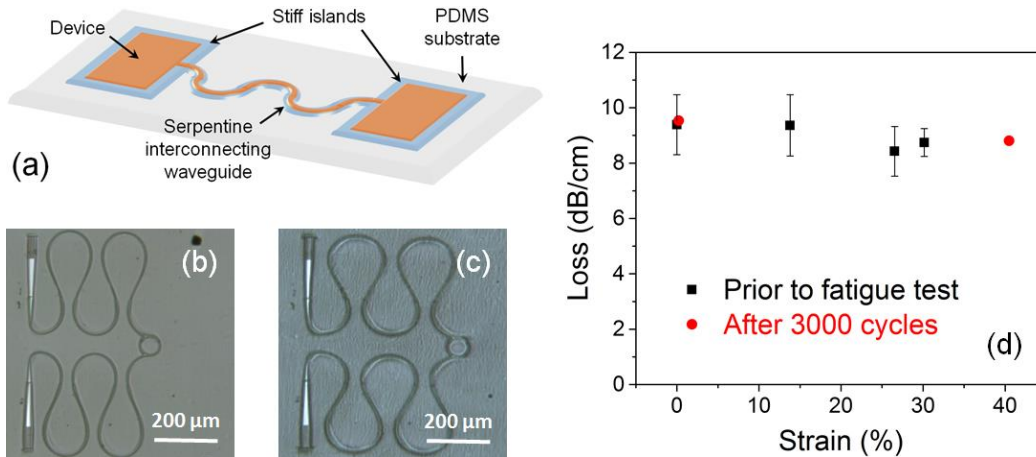


Fig. 4. (a) Schematic layout of an integrated photonic chip design to enable large stretchability while minimizing undesired strain-induced wavelength shift in critical optical devices; (b) & (c) top-view micrographs of a stretchable device (b) at 0% strain and (c) the same device at 36% tensile strain; (d) measured optical loss in a micro-resonator prior to and after a mechanical fatigue test consisting of 3,000 stretching cycles at 42% tensile strain [34].

Fig. 4a schematically illustrates the design concept of a stretchable photonic circuit, which comprises isolated stiff “islands” connected by stretchable optical waveguides. The design stabilizes device operation while maintaining large stretchability. Photonic components sensitive to geometry changes are located on the rigid “islands” in the form of lithographically patterned SU-8 pads and thereby minimizing their deformation. To transform SU-8 and Ge₂₃Sb₇S₇₀ glass, both brittle materials, into stretchable waveguide structures, we patterned both layers into a serpentine shape. The meandering geometry can withstand large tensile deformation without structural damage in a way similar to stretching a helix-shaped spring [44].

Fig. 4b shows a top-view optical microscope image of a prototypical stretchable device consisting of two grating couplers for input and output light coupling from optical fibers, a micro-ring resonator, and serpentine single-mode ChG waveguides connecting the components following the design in Fig. 4a. Since the operation wavelength of grating couplers critically depends on the grating period, the grating couplers are placed on SU-8 islands to prevent undesired strain-induced wavelength drift. The device is mounted on a home-built optical testing station to characterize its optical response in-situ while the device is strained. Fig. 4c shows the same device after applying a tensile strain (elongation) of 36% on the PDMS substrate clearly showing the in-plane deformation of the serpentine waveguides. Close optical microscopy inspection reveals that the device can sustain repeated stretching without cracking or damage. Fig. 4d plots the optical propagation loss in the micro-ring resonator measured at different strain states, both before and after a fatigue test consisting of 3,000 stretching cycles at 42% tensile strain. No measurable loss change was observed despite the large applied tensile strain. The result proves that mechanically robust stretchable photonic devices can be made from glass materials which are brittle in their bulk state, without degradation of optical performance. The general micro-mechanical design principles are equally applicable to other material systems, thereby enabling flexible and stretchable optical systems to be constructed out of a diverse range of materials regardless of their intrinsic mechanical behavior.

Active-passive photonic integration on flexible substrates

In the previous sections, we focus on flexible photonic systems containing only passive elements, such as optical waveguides, gratings, and resonators. A complete photonic integrated circuit (PIC) entails active optoelectronic devices such as light sources, modulators, switches and photodetectors interconnected by a waveguide network. We have therefore taken the first step towards a flexible PIC by demonstrating a waveguide-integrated nanomembrane photodetector. Compared to conventional normal incidence photodetectors which collect optical radiation incident from free-space, waveguide-integrated detectors are not only essential building blocks for PICs but also claim a number of performance advantages such as noise suppression and high-speed response [45, 46].

Glass again plays a pivotal role in this device: the waveguide that channels optical signals into the detector is made of $\text{Ge}_{23}\text{Sb}_7\text{S}_{70}$ chalcogenide glass. The flexible device fabrication process, which allows seamless integration of glass-based passive elements with semiconductor active devices, capitalizes on the substrate-agnostic, monolithic integration capability of ChGs: they can be deposited onto almost all technically important substrate materials, in this case polymers and semiconductor nanomembranes, without compromising their optical properties. The active-passive integration technology described herein can also be readily extended to incorporate other optoelectronic components including lasers.

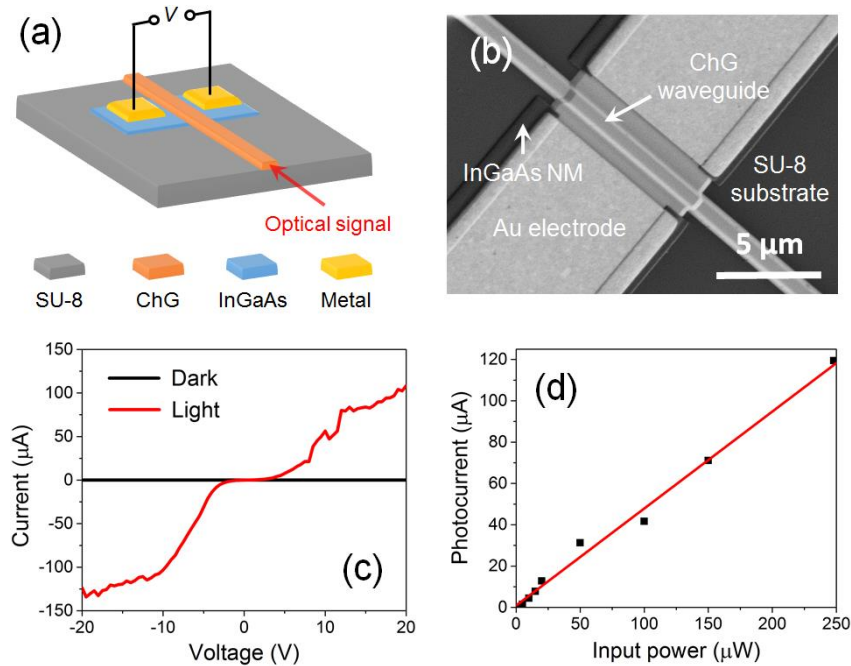


Fig. 5. (a) Schematic diagram of the glass waveguide-integrated photodetector; (b) SEM micrograph of a detector; (c) I-V response of the detector in dark and under illumination; (d) photocurrent of the detector as a function of input optical power in the waveguide.

The glass waveguide-integrated NM detector structure is schematically illustrated in Fig. 5a. The photodetector employs a lateral metal-semiconductor-metal (MSM) structure consisting of an InGaAs semiconductor nanomembrane optical absorber layer with a pair of gold electrodes juxtaposed on both sides of a ChG waveguide. Light propagating in the waveguide is directed to the InGaAs mesa and is absorbed by the semiconductor to create electron-hole pairs. When a voltage bias is applied across the two electrodes, the photo-generated charged carriers in InGaAs

can cross the Schottky barrier between the metal electrode and the semiconductor, leading to a photocurrent which scales with the incident light intensity.

The device was fabricated following the procedures below. An SU-8 layer is first spin coated on a handler wafer. An InP die with an epitaxially grown InGaAs layer is bonded onto the wafer with the epi-layer facing the substrate. The SU-8 film serves as an adhesive in the bonding process. The InP die is subsequently removed by mechanical lapping followed by wet chemical etching, leaving behind the InGaAs absorber NM of about 200 nm in thickness. The NM is lithographically patterned and wet etched to form the detector mesa. Glass waveguides and metal electrodes are then fabricated on top of the NM mesa to define the detector structure. In the last step, the flexible device supported by the SU-8 film is delaminated from the handler wafer. Fig. 5b presents an SEM micrograph of the completed device.

During testing, optical signal was launched into the waveguide from an optical fiber probe and the electrical response was monitored using a pair of micro-probes (Fig. 1f). The fabricated detector device was mounted on a motion stage during optoelectronic characterizations such that it can be mechanically buckled in-situ at varying bending radii. Fig. 5c plots the current-voltage (I-V) curves of the detector measured in dark and under illumination with 250 μ W incident optical power at 1550 nm wavelength. The device shows a negligible saturation dark current of 0.5 nA at 10 V bias. The photocurrent increases linearly with increasing optical power, as shown in Fig. 5d. Slope of the response curve yields a responsivity of 0.5 A/W at 1550 nm, corresponding to an external quantum efficiency of 40%. Our bending tests shows that dark current and photo response of the device remain unchanged with bending radii down to 0.7 mm, which represents a significant improvement in mechanical flexibility over previously demonstrated semiconductor NM photodetectors [47].

Summary

In this article, we provide an overview on glass-based flexible integrated photonics based on both ultra-thin glass substrates and hybrid polymer-glass device architectures. We illustrate through the examples of glass-based bendable and stretchable photonics that clever mechanical designs can lift constraints imposed on intrinsic mechanical properties of constituent materials in flexible systems, thereby allowing the creation of highly compliant device modules out of brittle materials including glass. Inorganic glasses, now formally introduced into the expanded material repertoire for flexible photonics, offer important performance edge compared to organic polymers, including significantly widened accessible range of optical properties, superior thermal and chemical stability, as well as highly versatile processing routes compatible with a diverse set of materials commonly used in photonic integration. We foresee that these useful attributes of glass materials for photonic integration, evidenced by our initial demonstration of flexible glass waveguide-integrated photodetectors, will ultimately pave the path towards a fully integrated flexible photonic circuitry.

Acknowledgements

Funding support for this work is provided by the National Science Foundation under awards 1453218 and 1506605, and the Department of Energy under grant DE-NA0002509. This work was performed in part at the Harvard University Center for Nanoscale Systems, a member of the National Nanotechnology Infrastructure Network (NNIN) supported by the National Science Foundation under award 0335765.

References

1. S. E. Miller, "Integrated optics: an introduction," *At&T Tech J* **48**, 2059-2069 (1969).
2. W. S. Wong and A. Salleo, *Flexible electronics: materials and applications* (Springer Science & Business Media, 2009), Vol. 11.
3. "Flexible Electronics Market By Component (Display, Battery, Sensors, and Memory) For Automotive, Consumer Electronics, Healthcare and Industrial Application: Global Industry Perspective, Comprehensive Analysis, Size, Share, Growth, Segment, Trends and Forecast, 2015 – 2021," (Zion Market Research, 2016).
4. D.-H. Kim, N. Lu, R. Ma, Y.-S. Kim, R.-H. Kim, S. Wang, J. Wu, S. M. Won, H. Tao, and A. Islam, "Epidermal electronics," *Science* **333**, 838-843 (2011).
5. S. Takeuchi, T. Suzuki, K. Mabuchi, and H. Fujita, "3D flexible multichannel neural probe array," *J Micromech Microeng* **14**, 104 (2003).
6. S. Aikio, J. Hiltunen, J. Hiitola-Keinänen, M. Hiltunen, V. Kontturi, S. Siitonen, J. Puustinen, and P. Karioja, "Disposable photonic integrated circuits for evanescent wave sensors by ultra-high volume roll-to-roll method," *Opt Express* **24**, 2527-2541 (2016).
7. S. Aikio, M. Zeilinger, J. Hiltunen, L. Hakalahti, J. Hiitola-Keinänen, M. Hiltunen, V. Kontturi, S. Siitonen, J. Puustinen, and P. Lieberzeit, "Disposable (bio) chemical integrated optical waveguide sensors implemented on roll-to-roll produced platforms," *RSC Advances* **6**, 50414-50422 (2016).
8. B. W. Swatowski, C. M. Amb, S. K. Breed, D. J. Deshazer, W. K. Weidner, R. F. Dangel, N. Meier, and B. J. Offrein, "Flexible, stable, and easily processable optical silicones for low loss polymer waveguides," in *SPIE OPTO*, (International Society for Optics and Photonics, 2013), 862205-862205-862211.
9. C. Choi, L. Lin, Y. Liu, J. Choi, L. Wang, D. Haas, J. Magera, and R. T. Chen, "Flexible optical waveguide film fabrications and optoelectronic devices integration for fully embedded board-level optical interconnects," *J Lightwave Technol* **22**, 2168 (2004).
10. E. Bosman, G. Van Steenberge, B. Van Hoe, J. Missinne, J. Vanfleteren, and P. Van Daele, "Highly reliable flexible active optical links," *Ieee Photonic Tech L* **22**, 287-289 (2010).
11. T.-J. Peters and M. Tichem, "Mechanically flexible waveguide arrays for optical chip-to-chip coupling," in *SPIE OPTO*, (International Society for Optics and Photonics, 2016), 97600D-97600D-97611.
12. L. Li, Y. Zou, H. T. Lin, J. J. Hu, X. C. Sun, N. N. Feng, S. Danto, K. Richardson, T. Gu, and M. Haney, "A Fully-Integrated Flexible Photonic Platform for Chip-to-Chip Optical Interconnects," *J Lightwave Technol* **31**, 4080-4086 (2013).
13. S. M. Kamali, A. Arbabi, E. Arbabi, Y. Horie, and A. Faraon, "Decoupling optical function and geometrical form using conformal flexible dielectric metasurfaces," *Nat Commun* **7**(2016).
14. H. C. Ko, M. P. Stoykovich, J. Song, V. Malyarchuk, W. M. Choi, C.-J. Yu, J. B. Geddes Iii, J. Xiao, S. Wang, and Y. Huang, "A hemispherical electronic eye camera based on compressible silicon optoelectronics," *Nature* **454**, 748-753 (2008).
15. L. Zhu, J. Kapraun, J. Ferrara, and C. J. Chang-Hasnain, "Flexible photonic metastructures for tunable coloration," *Optica* **2**, 255-258 (2015).
16. Y. Chen, H. Li, and M. Li, "Flexible and tunable silicon photonic circuits on plastic substrates," *arXiv preprint arXiv:1207.3748* (2012).
17. C. L. Yu, H. Kim, N. de Leon, I. W. Frank, J. T. Robinson, M. McCutcheon, M. Liu, M. D. Lukin, M. Loncar, and H. Park, "Stretchable photonic crystal cavity with wide frequency tunability," *Nano Lett* **13**, 248-252 (2012).
18. Y. Zou, L. Moreel, H. T. Lin, J. Zhou, L. Li, S. Danto, J. D. Musgraves, E. Koontz, K. Richardson, K. D. Dobson, R. Birkmire, and J. J. Hu, "Solution Processing and Resist-Free Nanoimprint Fabrication of Thin Film Chalcogenide Glass Devices: Inorganic-Organic Hybrid Photonic Integration," *Adv Opt Mater* **2**, 759-764 (2014).

19. J. P. Bristow, Y. Liu, T. Marta, S. Bounnak, K. Johnson, Y.-S. Liu, and H. S. Cole, "Cost-effective optoelectronic packaging for multichip modules and backplane level optical interconnects," in *Photonics West'95*, (International Society for Optics and Photonics, 1995), 61-73.
20. M. Hikita, R. Yoshimura, M. Usui, S. Tomaru, and S. Imamura, "Polymeric optical waveguides for optical interconnections," *Thin Solid Films* **331**, 303-308 (1998).
21. T. Matsuura, J. Kobayashi, S. Ando, T. Maruno, S. Sasaki, and F. Yamamoto, "Heat-resistant flexible-film optical waveguides from fluorinated polyimides," *Appl Optics* **38**, 966-971 (1999).
22. G. T. Palocz, Y. Huang, and A. Yariv, "Free-standing all-polymer microring resonator optical filter," *Electron Lett* **39**, 1650-1651 (2003).
23. H. Ma, A. Y. Jen, and L. R. Dalton, "Polymer - Based Optical Waveguides: Materials, Processing, and Devices," *Adv Mater* **14**, 1339-1365 (2002).
24. X. Xu, H. Subbaraman, A. Hosseini, C.-Y. Lin, D. Kwong, and R. T. Chen, "Stamp printing of silicon-nanomembrane-based photonic devices onto flexible substrates with a suspended configuration," *Opt Lett* **37**, 1020-1022 (2012).
25. W. Zhou, Z. Ma, H. Yang, Z. Qiang, G. Qin, H. Pang, L. Chen, W. Yang, S. Chuwongin, and D. Zhao, "Flexible photonic-crystal Fano filters based on transferred semiconductor nanomembranes," *Journal of Physics D: Applied Physics* **42**, 234007 (2009).
26. W. Zhou, Z. Ma, S. Chuwongin, Y.-C. Shuai, J.-H. Seo, D. Zhao, H. Yang, and W. Yang, "Semiconductor nanomembranes for integrated silicon photonics and flexible Photonics," *Optical and Quantum Electronics* **44**, 605-611 (2012).
27. A. Ghaffari, A. Hosseini, X. Xu, D. Kwong, H. Subbaraman, and R. T. Chen, "Transfer of micro and nano-photonic silicon nanomembrane waveguide devices on flexible substrates," *Opt Express* **18**, 20086-20095 (2010).
28. J. Hu, L. Li, H. Lin, P. Zhang, W. Zhou, and Z. Ma, "Flexible integrated photonics: where materials, mechanics and optics meet [Invited]," *Opt Mater Express* **3**, 1313-1331 (2013).
29. A. Plichta, A. Habeck, S. Knoche, A. Kruse, A. Weber, and N. Hildebrand, "Flexible glass substrates," *Flexible Flat Panel Displays* **3**, 35 (2005).
30. A. Plichta, A. Weber, and A. Habeck, "Ultra thin flexible glass substrates," in *MRS Proceedings*, (Cambridge Univ Press, 2003), H9. 1.
31. S. Huang, M. Li, S. M. Garner, M.-J. Li, and K. P. Chen, "Flexible photonic components in glass substrates," *Opt Express* **23**, 22532-22543 (2015).
32. J. Lapointe, Y. Ledemi, S. Loranger, V. L. Iezzi, E. S. de Lima Filho, F. Parent, S. Morency, Y. Messaddeq, and R. Kashyap, "Fabrication of ultrafast laser written low-loss waveguides in flexible As₂S₃ chalcogenide glass tape," *Opt Lett* **41**, 203-206 (2016).
33. J. J. Hu, L. Li, H. T. Lin, Y. Zou, Q. Y. Du, C. Smith, S. Novak, K. Richardson, and J. D. Musgraves, "Chalcogenide glass microphotonics: Stepping into the spotlight," *Am Ceram Soc Bull* **94**, 24-29 (2015).
34. L. Li, H. Lin, K. Wang, Y. Huang, J. Li, J. Michon, Q. Du, A. Yadav, K. Richardson, and J. Hu, "Monolithic stretchable integrated photonics," to be submitted (2016).
35. L. Li, H. T. Lin, S. Geiger, A. Zerdoum, P. Zhang, O. Ogbuu, Q. Y. Du, X. Q. Jia, S. Novak, C. Smith, K. Richardson, J. D. Musgraves, and J. J. Hu, "Amorphous thin films for mechanically flexible, multimaterial integrated photonics," *Am Ceram Soc Bull* **95**, 34-36 (2016).
36. N. Lu, S. Yang, and S. Qiao, "Mechanics of flexible electronics and photonics based on inorganic micro-and nanomaterials," in *SPIE Defense+ Security*, (International Society for Optics and Photonics, 2014), 90831J-90831J-90812.
37. L. Li, P. Zhang, W.-M. Wang, H. Lin, A. B. Zerdoum, S. J. Geiger, Y. Liu, N. Xiao, Y. Zou, and O. Ogbuu, "Foldable and Cytocompatible Sol-gel TiO₂ Photonics," *Sci Rep-Uk* **5**(2015).
38. L. Fan, L. T. Varghese, Y. Xuan, J. Wang, B. Niu, and M. Qi, "Direct fabrication of silicon photonic devices on a flexible platform and its application for strain sensing," *Opt Express* **20**, 20564-20575 (2012).

39. L. Li, H. Lin, S. Qiao, Y. Zou, S. Danto, K. Richardson, J. D. Musgraves, N. Lu, and J. Hu, "Integrated flexible chalcogenide glass photonic devices," *Nat Photonics* **8**, 643-649 (2014).
40. Y. Zou, D. Zhang, H. Lin, L. Li, L. Moreel, J. Zhou, Q. Du, O. Ogbuu, S. Danto, and J. D. Musgraves, "High - Performance, High - Index - Contrast Chalcogenide Glass Photonics on Silicon and Unconventional Non - planar Substrates," *Adv Opt Mater* **2**, 478-486 (2014).
41. J. Missinne, S. Kalathimekkad, B. Van Hoe, E. Bosman, J. Vanfleteren, and G. Van Steenberge, "Stretchable optical waveguides," *Opt Express* **22**, 4168-4179 (2014).
42. Y. Zou, H. Lin, O. Ogbuu, L. Li, S. Danto, S. Novak, J. Novak, J. D. Musgraves, K. Richardson, and J. Hu, "Effect of annealing conditions on the physio-chemical properties of spin-coated As₂Se₃ chalcogenide glass films," *Opt Mater Express* **2**, 1723-1732 (2012).
43. Q. Du, Y. Huang, J. Li, D. Kita, J. Michon, H. Lin, L. Li, S. Novak, K. Richardson, and W. Zhang, "Low-loss photonic device in Ge-Sb-S chalcogenide glass," *Opt Lett* **41**, 3090-3093 (2016).
44. D.-H. Kim, N. Lu, R. Ghaffari, Y.-S. Kim, S. P. Lee, L. Xu, J. Wu, R.-H. Kim, J. Song, and Z. Liu, "Materials for multifunctional balloon catheters with capabilities in cardiac electrophysiological mapping and ablation therapy," *Nat Mater* **10**, 316-323 (2011).
45. Z. Han, V. Singh, D. Kita, C. Monmeyran, P. Becla, P. Su, J. Li, X. Huang, L. Kimerling, and J. Hu, "On-chip chalcogenide glass waveguide-integrated mid-infrared PbTe detectors," *Appl Phys Lett* **109**, 071111 (2016).
46. D. Ahn, C.-y. Hong, J. Liu, W. Giziewicz, M. Beals, L. C. Kimerling, J. Michel, J. Chen, and F. X. Kärtner, "High performance, waveguide integrated Ge photodetectors," *Opt Express* **15**, 3916-3921 (2007).
47. W. Yang, H. Yang, G. Qin, Z. Ma, J. Berggren, M. Hammar, R. Soref, and W. Zhou, "Large-area InP-based crystalline nanomembrane flexible photodetectors," *Appl Phys Lett* **96**, 121107 (2010).